

Iterative Decoding and Phase-Noise Compensation for Multichannel Optical Transmission

Arni F. Alfredsson, Erik Agrell, *Fellow, IEEE*, and Henk Wymeersch, *Member, IEEE*

Abstract—The problem of phase-noise compensation for correlated phase noise in coded multichannel optical transmission is investigated. To that end, a multichannel phase-noise model is introduced and the maximum *a posteriori* detector for this model is approximated using two frameworks, namely factor graphs (FGs) and the sum-product algorithm (SPA), as well as a variational Bayesian (VB) inference. The resulting pilot-aided algorithms perform phase-noise compensation in cooperation with an iterative decoder, using extended Kalman smoothing to estimate the *a posteriori* phase-noise distribution jointly for all channels. Through Monte Carlo simulations, the algorithms are assessed in terms of phase-noise tolerance for coded transmission. It is observed that they significantly outperform the conventional approach of performing phase-noise compensation separately for each channel. Moreover, the results reveal that the FG/SPA framework performs similarly or better than the VB framework in terms of phase-noise tolerance of the resulting algorithms.

Index Terms—Phase noise, maximum *a posteriori*, detection, estimation, inference, factor graphs, sum product algorithm, variational Bayesian.

I. INTRODUCTION

Phase noise is an inherent problem in optical communications. This comes due to the nonzero linewidth of light sources and local oscillators (LOs) [1], and can have devastating effects on the system performance if not handled properly. This is particularly relevant since focus has shifted in recent years towards high-order quadrature amplitude modulation (QAM) or more advanced multilevel modulation formats [2]. In general, systems become more sensitive to phase noise as the modulation order grows, and hence, effective phase-noise compensation becomes crucial. Traditionally, phase-noise compensation methods in optical communication have been blind, i.e., they do not use pilot symbols to assist with the estimation, and thus, spectral efficiency is not sacrificed. Well-known examples are the Viterbi–Viterbi algorithm [3] and blind phase search (BPS) [4]. However, blind methods suffer from ambiguity in the phase-noise estimation and are therefore susceptible to cycle slips, which result in burst errors [5] that can not be corrected with a code. This can be handled with differential encoding, which has the downside of increasing the average bit error rate (BER). Alternatively, one can resort to pilot-aided phase-noise estimation.

Recently, space-division multiplexing (SDM) has been a topic of particular interest. It involves the integration of various

system components, such as optical hardware and digital signal processing (DSP) modules, as well as the utilization of multicore and multimode fibers, combinations thereof, or bundles of single-mode fibers [6]. These systems enable the joint-channel compensation of various signal impairments, in particular phase noise, as light sources and LOs can be shared between different cores or modes [7]. This gives rise to spatial correlation in the phase noise, which can be exploited to relax hardware requirements [8] and reduce receiver complexity [9]. However, the phase noise is not perfectly correlated, as environmental effects and system imperfections introduce phase drifts between cores and polarizations [7], [10].

On a related note, transmission using frequency combs has shown a similar potential for phase-noise compensation, as frequency combs enable phase locking between the different frequency lines. However, similarly to SDM systems, the phase noise is not perfectly correlated among the spectral channels, due to imperfections in the comb generation [11]. Joint-channel phase-noise compensation has also been demonstrated in systems utilizing electrically generated subcarriers [12]. Thus, there are various types of optical systems where joint-channel phase-noise compensation has potential and ought to be investigated.

Multiple solutions that exploit the phase-noise correlation between channels have been proposed for SDM and frequency comb systems. The majority has focused on master-slave schemes [7], [11]–[13], in which one channel is used to produce phase-noise estimates that are used to compensate for all channels. While this reduces DSP complexity, the phase-noise correlation can also be used to improve performance in terms of increased phase-noise tolerance or, in the case of pilot-aided schemes, lower the pilot rate while maintaining the phase-noise tolerance.

Wireless communication faces a similar problem with oscillator phase noise, which has given rise to a myriad of solutions that approximate the maximum *a posteriori* (MAP) detector for phase-noise channels. In particular, various iterative algorithms that perform phase-noise compensation and data detection have been proposed. Pertaining to single-channel transmission, iterative solutions have been developed based on factor graphs (FGs) and the sum-product algorithm (SPA) [14]–[16], variational Bayesian (VB) inference [17], and the expectation-maximization algorithm [18], [19]. Moreover, in the context of multiple-input multiple-output (MIMO) systems for wireless transmission, various methods have been proposed for joint-channel phase-noise compensation [20]. In [21], [22], several algorithms are proposed for joint phase-noise estimation and data detection using the aforementioned frame-

Arni F. Alfredsson, Erik Agrell, and Henk Wymeersch are with the Department of Electrical Engineering, Chalmers University of Technology, SE-41296 Göteborg, Sweden (e-mail: arnia@chalmers.se; agrell@chalmers.se; henkw@chalmers.se).

This work was supported by the Swedish Research Council (VR) under Grants 2013-5642 and 2014-6138.

works, and in [23], joint channel and phase-noise estimation for MIMO systems is proposed. These methods assume that the oscillator phase noise is either identical or independent between channels in the MIMO system, which are limiting assumptions for the scenario of interest in this work.

In this paper, we propose algorithms for joint phase-noise estimation and data detection for multichannel transmission using Bayesian frameworks and techniques, which has not been done in the context of optical communication. We introduce a multichannel system model that describes correlated phase noise, which we then use to develop two algorithms using FGs and the SPA [24], as well as VB inference [25]. Finally, we assess the algorithms for coded transmission in terms of phase-noise tolerance.

Notation: Real and imaginary parts of a complex number are denoted with $\Re\{\cdot\}$ and $\Im\{\cdot\}$, resp. Moreover, $(\cdot)^*$ and $\angle(\cdot)$ are the complex conjugate and angle of a complex number. Random variables and their realizations are denoted with X and x , resp. Probability density functions (PDFs) and probability mass functions (PMFs) are written as $p(x)$ and $P(x)$, resp. In particular, a Gaussian PDF with mean $\boldsymbol{\mu}$, covariance matrix $\boldsymbol{\Sigma}$, and argument \mathbf{z} is denoted with $\mathcal{N}_{\mathbf{z}}(\boldsymbol{\mu}, \boldsymbol{\Sigma})$, whereas a Tikhonov PDF with a complex parameter κ and argument \mathbf{z} is denoted with $\mathcal{T}_{\mathbf{z}}(\kappa)$. Scalars, vectors, and matrices are typeset as x , \mathbf{x} , and \mathbf{X} , resp. A diagonal matrix is denoted with $\text{diag}(\cdot)$, whereas the identity matrix of size D is written as \mathbf{I}_D . Finally, the vector transpose is denoted with $(\cdot)^T$.

II. SYSTEM MODEL

Transmission over D parallel channels is considered. The transmitted symbol block, i.e., frames, in each channel is modelled as a vector of N random variables, where every random variable is drawn uniformly from a set \mathcal{X} of constellation points. The constellation is normalized such that the mean of the constellation points is zero and the average symbol energy is E_s . As phase-noise compensation is normally one of the last stages in the DSP chain [26], [27], all signal distortions are assumed to have been perfectly compensated for with the exception of phase noise and additive white Gaussian noise (AWGN). Further assuming one sample per symbol, the discrete-time baseband model is written as

$$r_{i,k} = s_{i,k} e^{j\gamma_{i,k}} + n_{i,k}, \quad (1)$$

where $k = 1, \dots, N$ is a time index and $i = 1, \dots, D$ is a channel index. The received samples, transmitted symbols, phase noise, and AWGN realizations are denoted with $r_{i,k}$, $s_{i,k}$, $\gamma_{i,k}$, and $n_{i,k}$, resp., where the AWGN on channel i has variance σ_i^2 . The vector $\mathbf{r}_k \triangleq [r_{1,k}, \dots, r_{D,k}]^T \in \mathbb{C}^D$ contains the received samples in all channels at time k , and the vectors \mathbf{s}_k , $\boldsymbol{\gamma}_k$, and \mathbf{n}_k are defined analogously. Finally, let \mathbf{r} contain all received samples, and \mathbf{s} , $\boldsymbol{\gamma}$, and \mathbf{n} be defined similarly.

The phase noise is assumed to be correlated across channels and time, and is thus modelled as a Gaussian multidimensional random walk, described by

$$\boldsymbol{\gamma}_k = \boldsymbol{\gamma}_{k-1} + \Delta\boldsymbol{\gamma}_k, \quad (2)$$

where $\boldsymbol{\gamma}_0$ is uniformly distributed on $[0, 2\pi)^D$ and $\Delta\boldsymbol{\gamma}_k$ is a multivariate zero-mean Gaussian random variable with

covariance matrix \mathbf{Q} . Furthermore, the phase noise is assumed to be independent from the transmitted symbols and AWGN, and unknown to both the transmitter and receiver. Finally, \mathbf{Q} and $\boldsymbol{\sigma}^2 \triangleq (\sigma_1^2, \dots, \sigma_D^2)$ are assumed known to the receiver.

The transmitted symbol sequence \mathbf{s} is assumed to be a codeword of length ND , obtained from encoding an information bit sequence \mathbf{b} of length N_b . Additional pilot symbols that are used for the phase-noise compensation are considered as a part of the channel code. The pilot and data distributions, $\mathcal{P} \triangleq \{(i, k) \in (1, \dots, D) \times (1, \dots, N) : s_{i,k} \text{ is known}\}$ and $\mathcal{D} \triangleq (1, \dots, D) \times (1, \dots, N) \setminus \mathcal{P}$, are assumed known to the transmitter and receiver.

III. DERIVATION OF ALGORITHMS

The MAP detector yields the lowest possible BER out of all detectors [28, Ch. 1.4]. It performs detection on a bit-by-bit basis according to

$$\hat{b}_l = \underset{b_l \in \{0,1\}}{\text{argmax}} P(b_l | \mathbf{r}), \quad (3)$$

for $l = 1, \dots, N_b$, where $P(b_l | \mathbf{r})$ is the *a posteriori* PMF of b_l . However, the PMF in (3) is hard to compute exactly for the system model in (1), and thus, approximations are needed. To that end, note that the desired PMF in (3) can be obtained through the marginalization

$$P(b_l | \mathbf{r}) = \int_{\mathcal{T}} \sum_{\mathbf{b} \in \mathcal{B}} p(\mathbf{b}, \boldsymbol{\gamma} | \mathbf{r}) d\boldsymbol{\gamma}, \quad (4)$$

where $\mathcal{T} = \mathbb{R}^{D \times N}$ and $\mathcal{B} = \{\mathbf{b}' \in \{0,1\}^{N_b} : b'_l = b_l\}$. To carry out this marginalization approximately but efficiently, we make use of two frameworks, namely FGs and the SPA, and VB inference.

Before applying these two frameworks, we derive the recursive equations used to approximately estimate the marginal *a posteriori* phase-noise PDFs, $p(\boldsymbol{\gamma}_k | \mathbf{r})$, for $k = 1, \dots, N$. This is done through two recursive passes; a forward pass with an extended Kalman filter (EKF) [29, Ch. 5.2] and a backward pass with a Rauch-Tung-Striebel smoother (RTSS) [29, Ch. 8.2]. The recursive equations provided by the EKF and RTSS are used by both frameworks to yield the final algorithms. The justification for utilizing an EKF is that the linearization imposed by the EKF on the system model works effectively, provided that the phase noise does not vary too rapidly. For laser linewidths up to a few MHz and symbol rates on the order of Gbaud, this is indeed the case, as will be evident by the performance results in Section IV.

A. EKF and RTSS Application to System Model

In this subsection, $s_{i,k}$ is assumed to be known for all (i, k) , and hence,

$$p(r_{i,k} | \boldsymbol{\gamma}_{i,k}) = \mathcal{N}_{r_{i,k}}(s_{i,k} e^{j\boldsymbol{\gamma}_{i,k}}, \sigma_i^2). \quad (5)$$

As $s_{i,k}$ is not known for $(i, k) \in \mathcal{D}$, a soft estimate of $s_{i,k}$ is used instead when the aforementioned frameworks are used in the following subsections. The general EKF equations can be

simplified for the system model in (1). They can be derived from the general recursive filtering equations [29, Ch. 4.2]

$$\begin{aligned} & p(\boldsymbol{\gamma}_k | \mathbf{r}_1, \dots, \mathbf{r}_k) \\ & \propto p(\mathbf{r}_k | \boldsymbol{\gamma}_k) \int_{\mathbb{R}^D} p(\boldsymbol{\gamma}_k | \boldsymbol{\gamma}_{k-1}) p(\boldsymbol{\gamma}_{k-1} | \mathbf{r}_1, \dots, \mathbf{r}_{k-1}) d\boldsymbol{\gamma}_{k-1}, \end{aligned} \quad (6)$$

for $k = 2, \dots, N$. Conforming to the EKF, the received samples in (1) are then linearized around an estimate of $\boldsymbol{\gamma}_{k-1}$, denoted with $\hat{\boldsymbol{\gamma}}_{k-1}^f$, using a first-order Taylor expansion as

$$r_{i,k} \approx s_{i,k} e^{j\hat{\gamma}_{i,k-1}^f} (1 + j(\gamma_{i,k} - \hat{\gamma}_{i,k-1}^f)) + n_{i,k}. \quad (7)$$

This yields

$$\begin{aligned} & p(\mathbf{r}_k | \boldsymbol{\gamma}_k) \\ & = \prod_{i=1}^D p(r_{i,k} | \gamma_{i,k}) \end{aligned} \quad (8)$$

$$= \prod_{i=1}^D \mathcal{N}_{r_{i,k}}(s_{i,k} e^{j\gamma_{i,k}}, \sigma_i^2) \quad (9)$$

$$\approx \prod_{i=1}^D \mathcal{N}_{r_{i,k}}(s_{i,k} e^{j\hat{\gamma}_{i,k-1}^f} (1 + j(\gamma_{i,k} - \hat{\gamma}_{i,k-1}^f)), \sigma_i^2) \quad (10)$$

$$\propto \prod_{i=1}^D \exp\left(-\frac{|s_{i,k}|^2}{2\sigma_i^2} |j + \hat{\gamma}_{i,k-1}^f + \eta_{i,k} - \gamma_{i,k}|^2\right) \quad (11)$$

$$\propto \prod_{i=1}^D \exp\left(-\frac{|s_{i,k}|^2}{2\sigma_i^2} (\hat{\gamma}_{i,k-1}^f + \Re\{\eta_{i,k}\} - \gamma_{i,k})^2\right) \quad (12)$$

$$\propto \prod_{i=1}^D \mathcal{N}_{\gamma_{i,k}}\left(\hat{\gamma}_{i,k-1}^f + \Im\left\{\frac{r_{i,k} e^{-j\hat{\gamma}_{i,k-1}^f}}{s_{i,k}}\right\}, \frac{|s_{i,k}|^2}{\sigma_i^2}\right), \quad (13)$$

where $\eta_{i,k} \triangleq r_{i,k} e^{-j\hat{\gamma}_{i,k-1}^f} / (j s_{i,k})$ and $\hat{\gamma}_{i,k-1}^f$ is the i th element of $\hat{\boldsymbol{\gamma}}_{k-1}^f$. Furthermore, (12) is obtained by using $|z|^2 = \Re\{z\}^2 + \Im\{z\}^2$, for $z \in \mathbb{C}$, as

$$\begin{aligned} & |j + \hat{\gamma}_{i,k-1}^f + \eta_{i,k} - \gamma_{i,k}|^2 \\ & = (1 + \Im\{\eta_{i,k}\})^2 + (\hat{\gamma}_{i,k-1}^f + \Re\{\eta_{i,k}\} - \gamma_{i,k})^2. \end{aligned} \quad (14)$$

The first term in (14) is constant with respect to $\gamma_{i,k}$ and can thus be discarded. Finally, (13) is obtained since $\Re\{z/j\} = \Im\{z\}$ for $z \in \mathbb{C}$, and therefore, $p(\mathbf{r}_k | \boldsymbol{\gamma}_k)$ can be expressed as

$$p(\mathbf{r}_k | \boldsymbol{\gamma}_k) \approx \mathcal{N}_{\mathbf{r}_k}(\hat{\boldsymbol{\gamma}}_{k-1}^f + \mathbf{g}_k, \mathbf{S}_k^{-1}), \quad (15)$$

where

$$\mathbf{S}_k = \text{diag}\left(\frac{|s_{1,k}|^2}{\sigma_1^2}, \dots, \frac{|s_{D,k}|^2}{\sigma_D^2}\right), \quad (16)$$

and $\mathbf{g}_k \triangleq [g_{1,k}, \dots, g_{D,k}]^T$ represents the estimated difference between $\boldsymbol{\gamma}_k$ and $\boldsymbol{\gamma}_{k-1}$, with each of its elements computed as

$$g_{i,k} = \Im\left\{\frac{r_{i,k} e^{-j\hat{\gamma}_{i,k-1}^f}}{s_{i,k}}\right\}. \quad (17)$$

Finally, using the following identity for the product of two Gaussians [30],

$$\mathcal{N}_{\mathbf{x}}(\mathbf{a}, \mathbf{A}) \mathcal{N}_{\mathbf{x}}(\mathbf{b}, \mathbf{B}) = \mathcal{N}_{\mathbf{b}}(\mathbf{a}, \mathbf{A} + \mathbf{B}) \mathcal{N}_{\mathbf{x}}(\mathbf{c}, \mathbf{C}), \quad (18)$$

where

$$\mathbf{T} = (\mathbf{I} + \mathbf{A}\mathbf{B}^{-1})^{-1}, \quad (19)$$

$$\mathbf{C} = \mathbf{T}\mathbf{A}, \quad (20)$$

$$\mathbf{c} = \mathbf{T}\mathbf{a} + \mathbf{T}\mathbf{A}\mathbf{B}^{-1}\mathbf{b}. \quad (21)$$

(6) can be reduced to

$$\begin{aligned} & p(\boldsymbol{\gamma}_k | \mathbf{r}_1, \dots, \mathbf{r}_k) \\ & \approx \mathcal{N}_{\boldsymbol{\gamma}_k}(\hat{\boldsymbol{\gamma}}_{k-1}^f + \mathbf{g}_k, \mathbf{S}_k^{-1}) \int_{\mathbb{R}^D} \mathcal{N}_{\boldsymbol{\gamma}_{k-1}}(\boldsymbol{\gamma}_k, \mathbf{Q}) \\ & \quad \cdot \mathcal{N}_{\boldsymbol{\gamma}_{k-1}}(\hat{\boldsymbol{\gamma}}_{k-1}^f, \mathbf{M}_{k|k-1}^f) d\boldsymbol{\gamma}_{k-1} \\ & = \mathcal{N}_{\boldsymbol{\gamma}_k}(\hat{\boldsymbol{\gamma}}_{k-1}^f + \mathbf{g}_k, \mathbf{S}_k^{-1}) \mathcal{N}_{\boldsymbol{\gamma}_k}(\hat{\boldsymbol{\gamma}}_{k-1}^f, \mathbf{M}_{k|k-1}^f) \\ & \propto \mathcal{N}_{\boldsymbol{\gamma}_k}(\mathbf{T}_k \hat{\boldsymbol{\gamma}}_{k-1}^f + \mathbf{T}_k \mathbf{M}_{k|k-1}^f \mathbf{S}_k (\hat{\boldsymbol{\gamma}}_{k-1}^f + \mathbf{g}_k), \mathbf{T}_k \mathbf{M}_{k|k-1}^f) \\ & = \mathcal{N}_{\boldsymbol{\gamma}_k}(\hat{\boldsymbol{\gamma}}_{k-1}^f + \mathbf{M}_{k|k-1}^f \mathbf{h}_k, \mathbf{M}_k^f), \end{aligned} \quad (22)$$

where $\mathbf{T}_k \triangleq (\mathbf{I}_D + \mathbf{M}_{k|k-1}^f \mathbf{S}_k)^{-1}$, and (22) is obtained since the integral of a PDF is one.

As a result, the PDFs $p(\boldsymbol{\gamma}_k | \mathbf{r}_1, \dots, \mathbf{r}_k)$, can be estimated for $k = 2, \dots, N$ with the following recursive equations, which can be regarded as a special case of the EKF:

$$\mathbf{M}_{k|k-1}^f = \mathbf{M}_{k-1}^f + \mathbf{Q}, \quad (24)$$

$$\mathbf{M}_k^f = (\mathbf{I}_D + \mathbf{M}_{k|k-1}^f \mathbf{S}_k)^{-1} \mathbf{M}_{k|k-1}^f, \quad (25)$$

$$\hat{\boldsymbol{\gamma}}_k^f = \hat{\boldsymbol{\gamma}}_{k-1}^f + \mathbf{M}_{k|k-1}^f \mathbf{h}_k, \quad (26)$$

with initial conditions

$$\hat{\boldsymbol{\gamma}}_1^f = [\angle(r_{1,1}(s_{1,1})^*), \dots, \angle(r_{D,1}(s_{D,1})^*)]^T, \quad (27)$$

$$\mathbf{M}_1^f = \text{diag}(\sigma_1^2, \dots, \sigma_D^2). \quad (28)$$

Moreover, \mathbf{Q} is the covariance matrix of the Gaussian increments in (2), whereas $\hat{\boldsymbol{\gamma}}_{k-1}^f$ denotes an estimate of $\boldsymbol{\gamma}_{k-1}$ based on all received samples up to and including time $k-1$. Finally, each component of $\mathbf{h}_k \triangleq [h_{1,k}, \dots, h_{D,k}]^T$ in (26) is computed as

$$h_{i,k} = \frac{1}{\sigma_i^2} \Im\left\{r_{i,k}(s_{i,k})^* e^{-j\hat{\gamma}_{i,k-1}^f}\right\}. \quad (29)$$

Furthermore, to estimate $p(\boldsymbol{\gamma}_k | \mathbf{r}) = p(\boldsymbol{\gamma}_k | \mathbf{r}_1, \dots, \mathbf{r}_N)$, the RTSS can be used [29, Ch. 8.2]. The associated recursive equations are given by

$$\mathbf{A}_k = \mathbf{M}_k^f (\mathbf{M}_{k+1|k}^f)^{-1}, \quad (30)$$

$$\hat{\boldsymbol{\gamma}}_k^s = \hat{\boldsymbol{\gamma}}_k^f + \mathbf{A}_k (\hat{\boldsymbol{\gamma}}_{k+1}^s - \hat{\boldsymbol{\gamma}}_k^f), \quad (31)$$

$$\mathbf{M}_k^s = \mathbf{M}_k^f + \mathbf{A}_k (\mathbf{M}_{k+1}^s - \mathbf{M}_{k+1|k}^f) \mathbf{A}_k^T, \quad (32)$$

for $k = N-1, N-2, \dots, 1$, with initial conditions

$$\hat{\boldsymbol{\gamma}}_N^s = \hat{\boldsymbol{\gamma}}_N^f, \quad (33)$$

$$\mathbf{M}_N^s = \mathbf{M}_N^f. \quad (34)$$

Thus, the parameters $\hat{\boldsymbol{\gamma}}_k^s$ and \mathbf{M}_k^s represent the mean vector and covariance matrix of the Gaussian approximation of $p(\boldsymbol{\gamma}_k | \mathbf{r})$, i.e.,

$$p(\boldsymbol{\gamma}_k | \mathbf{r}) \approx \mathcal{N}_{\boldsymbol{\gamma}_k}(\hat{\boldsymbol{\gamma}}_k^s, \mathbf{M}_k^s). \quad (35)$$

The EKF and RTSS equations are summarized in Algorithm 1, where $\{(\hat{\boldsymbol{\gamma}}_k^s, \mathbf{M}_k^s)\}$ denotes the set of $(\hat{\boldsymbol{\gamma}}_k^s, \mathbf{M}_k^s)$ for all k .

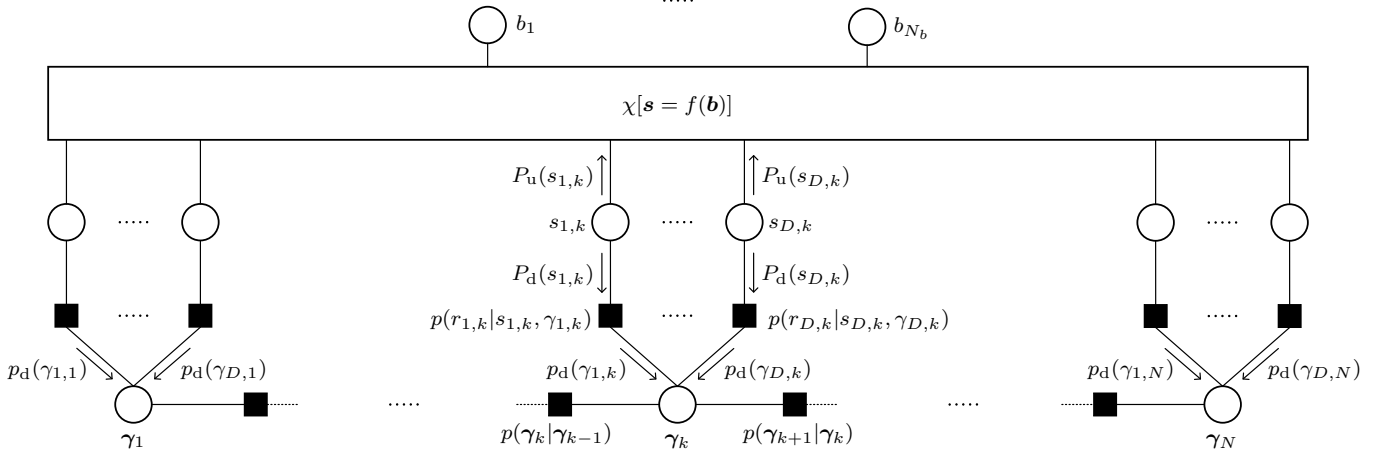


Fig. 1. A part of the FG corresponding to (38).

Algorithm 1 EKF/RTSS

Input: $\mathbf{r}, \mathbf{s}, D, N, \mathbf{Q}, \sigma^2$

Output: $\{(\hat{\gamma}_k^s, \mathbf{M}_k^s)\}$

- 1: $\hat{\gamma}_1^f = [\angle(r_{1,1}s_{1,1}^*), \dots, \angle(r_{D,1}s_{D,1}^*)]^T$
- 2: $\mathbf{M}_1^f = \text{diag}(\sigma_1^2, \dots, \sigma_D^2)$
- 3: **for** $k = 2, \dots, N$ **do**
- 4: **for** $i = 1, \dots, D$ **do**
- 5: $h_{i,k} = \Im\{r_{i,k}s_{i,k}^* e^{-j\hat{\gamma}_{i,k-1}^f}\}/\sigma_i^2$
- 6: **end for**
- 7: $\mathbf{S}_k = \text{diag}(|s_{1,k}|^2/\sigma_1^2, \dots, |s_{D,k}|^2/\sigma_D^2)$
- 8: $\mathbf{M}_{k|k-1}^f = \mathbf{M}_{k-1}^f + \mathbf{Q}$
- 9: $\mathbf{M}_k^f = (\mathbf{I}_D + \mathbf{M}_{k|k-1}^f \mathbf{S}_k)^{-1} \mathbf{M}_{k|k-1}^f$
- 10: $\hat{\gamma}_k^f = \hat{\gamma}_{k-1}^f + \mathbf{M}_k^f \mathbf{h}_k$
- 11: **end for**
- 12: $\hat{\gamma}_N^s = \hat{\gamma}_N^f$
- 13: $\mathbf{M}_N^s = \mathbf{M}_N^f$
- 14: **for** $k = N-1, N-2, \dots, 1$ **do**
- 15: $\mathbf{A}_k = \mathbf{M}_k^f (\mathbf{M}_{k+1}^f)^{-1}$
- 16: $\hat{\gamma}_k^s = \hat{\gamma}_k^f + \mathbf{A}_k (\hat{\gamma}_{k+1}^s - \hat{\gamma}_k^f)$
- 17: $\mathbf{M}_k^s = \mathbf{M}_k^f + \mathbf{A}_k (\mathbf{M}_{k+1}^s - \mathbf{M}_{k+1}^f) \mathbf{A}_k^T$
- 18: **end for**

B. FG/SPA-Based Algorithm

We assume that the reader is familiar with FGs and the SPA. If not, [24] gives a thorough introduction to the topic. The joint distribution $p(\mathbf{b}, \boldsymbol{\gamma}|\mathbf{r})$ in (4) may be factorized as

$$p(\mathbf{b}, \boldsymbol{\gamma}|\mathbf{r}) = \chi[\mathbf{s} = f(\mathbf{b})]p(\mathbf{s}, \boldsymbol{\gamma}|\mathbf{r}) \quad (36)$$

$$\propto \chi[\mathbf{s} = f(\mathbf{b})]p(\mathbf{r}|\mathbf{s}, \boldsymbol{\gamma})p(\boldsymbol{\gamma}) \quad (37)$$

$$\propto \chi[\mathbf{s} = f(\mathbf{b})] \prod_{(i,k)} p(r_{i,k}|s_{i,k}, \gamma_{i,k}) \prod_k p(\boldsymbol{\gamma}_k|\boldsymbol{\gamma}_{k-1}), \quad (38)$$

for $i = 1, \dots, D$ and $k = 1, \dots, N$, where $\chi[\mathbf{s} = f(\mathbf{b})]$ is the code indicator function [24], i.e., 1 if \mathbf{s} is equal to a codeword and 0 otherwise, and $f(\cdot)$ is the encoding function of the code. Furthermore, $p(r_{i,k}|s_{i,k}, \gamma_{i,k})$ is the likelihood function of $s_{i,k}$ from the channel, and $p(\boldsymbol{\gamma}_k|\boldsymbol{\gamma}_{k-1}) = \mathcal{N}_{\boldsymbol{\gamma}_k}(\boldsymbol{\gamma}_{k-1}, \mathbf{Q})$.

The FG associated with (38) is shown partly in Fig. 1. In case of coded transmission where an iterative decoder is utilized, e.g., for low-density parity-check (LDPC) codes and turbo codes, applying the SPA to this FG will yield an iterative phase-noise estimation and decoding algorithm, where in each iteration, the message $P_d(s_{i,k})$ corresponds to the extrinsic information about $s_{i,k}$ given by the decoder. Moreover, $P_u(s_{i,k})$ can be regarded as the likelihood function of $s_{i,k}$ from a virtual memoryless phase-noise compensated channel. It can be expressed as

$$\begin{aligned} P_u(s_{i,k}) &\propto \int_{\mathcal{T}} p(r_{i,k}|s_{i,k}, \gamma_{i,k}) \prod_{l=1}^N p(\boldsymbol{\gamma}_l|\boldsymbol{\gamma}_{l-1}) \\ &\quad \cdot \prod_{o \neq i} p_d(\boldsymbol{\gamma}_{o,k}) \prod_{l \neq k} \prod_{j=1}^D p_d(\boldsymbol{\gamma}_{j,l}) d\boldsymbol{\gamma} \\ &\propto \int_{\mathcal{T}} p(r_{i,k}|s_{i,k}, \gamma_{i,k}) \frac{p(\boldsymbol{\gamma})}{p_d(\boldsymbol{\gamma}_{i,k})} \prod_{j,l} p_d(\boldsymbol{\gamma}_{j,l}) d\boldsymbol{\gamma} \\ &\propto \int_{\mathcal{T}} p(r_{i,k}|s_{i,k}, \gamma_{i,k}) \frac{p(\boldsymbol{\gamma})}{p(r_{i,k}|\boldsymbol{\gamma}_{i,k})} \prod_{j,l} p(r_{j,l}|\boldsymbol{\gamma}_{j,l}) d\boldsymbol{\gamma} \\ &\propto \int_{\mathcal{T}} p(r_{i,k}|s_{i,k}, \gamma_{i,k}) \frac{p(\boldsymbol{\gamma})p(\mathbf{r}|\boldsymbol{\gamma})}{p(r_{i,k}|\boldsymbol{\gamma}_{i,k})} d\boldsymbol{\gamma} \\ &\propto \int_{\mathbb{R}^D} p(r_{i,k}|s_{i,k}, \gamma_{i,k}) \frac{p(\boldsymbol{\gamma}_k|\mathbf{r})}{p(r_{i,k}|\boldsymbol{\gamma}_{i,k})} d\boldsymbol{\gamma}_k. \end{aligned} \quad (39)$$

The expression in (39) can be solved in closed form through the utilization of the EKF and RTSS, and the message $P_u(s_{i,k})$ is converted to bit-wise log-likelihood ratios (LLRs) [28] that are fed to decoder. The decoder then either outputs the detected information bits or *a posteriori* LLRs of the coded bits, which are converted to $P_u(s_{i,k})$.

Note that for uncoded transmission, $P_d(s_{i,k})$ is simply the *a priori* PMF of $s_{i,k}$, and since the FG corresponding to (38) does not contain any cycles in the absence of a code [21], the algorithm that results from applying the SPA will not be iterative and, as the information bits are equiprobable, $P_u(s_{i,k})$ is used to detect the symbols, followed by symbol-to-bit demapping.

The message $p_d(\gamma_{i,k})$ is a Gaussian mixture, since

$$p_d(\gamma_{i,k}) = p(r_{i,k}|\gamma_{i,k}) \quad (40)$$

$$= \sum_{s_{i,k} \in \mathcal{X}} P_d(s_{i,k}) p(r_{i,k}|s_{i,k}, \gamma_{i,k}) \quad (41)$$

$$= \sum_{s_{i,k} \in \mathcal{X}} P_d(s_{i,k}) \mathcal{N}_{r_{i,k}}(s_{i,k} e^{j\gamma_{i,k}}, \sigma_i^2). \quad (42)$$

To ensure efficient message passing, the same approach is taken as in [14], i.e., $p_d(\gamma_{i,k})$ is approximated as a single Gaussian, with mean and variance chosen such that the Kullback-Leibler (KL) divergence between $p_d(\gamma_{i,k})$ and the single Gaussian is minimized [31]. This yields

$$p_d(\gamma_{i,k}) \approx \mathcal{N}_{r_{i,k}}(\bar{s}_{i,k} e^{j\gamma_{i,k}}, \bar{\sigma}_{i,k}^2), \quad (43)$$

where

$$\bar{s}_{i,k} \triangleq \sum_{s_{i,k} \in \mathcal{X}} s_{i,k} P_d(s_{i,k}), \quad (44)$$

$$\bar{\sigma}_{i,k}^2 \triangleq \sigma_i^2 + \sum_{s_{i,k} \in \mathcal{X}} |s_{i,k} - \bar{s}_{i,k}|^2 P_d(s_{i,k}). \quad (45)$$

The second term in (45) corresponds to the variance of $s_{i,k}$ with respect to $P_d(s_{i,k})$. For pilot symbols, $\bar{s}_{i,k} = s_{i,k}$ and $\bar{\sigma}_{i,k}^2 = \sigma_i^2$, whereas for information symbols, $\bar{s}_{i,k}$ and $\bar{\sigma}_{i,k}^2$ are initialized as $\bar{s}_{i,k} = 0$ and $\bar{\sigma}_{i,k}^2 = \sigma_i^2 + E_s$. The marginal *a posteriori* phase-noise PDFs, $p(\gamma_k|\mathbf{r})$, can then be approximated as multivariate Gaussian distributions and estimated using Algorithm 1. Due to the approximation in (43), \mathbf{S}_k in (25) and each component of \mathbf{h}_k in (26) are now computed as

$$\mathbf{S}_k = \text{diag}\left(\frac{|\bar{s}_{1,k}|^2}{\bar{\sigma}_{1,k}^2}, \dots, \frac{|\bar{s}_{D,k}|^2}{\bar{\sigma}_{D,k}^2}\right), \quad (46)$$

$$h_{i,k} = \frac{1}{\bar{\sigma}_{i,k}^2} \Im\left\{r_{i,k} \bar{s}_{i,k}^* e^{-j\hat{\gamma}_{i,k-1}^f}\right\}, \quad (47)$$

and the EKF equations are initialized with

$$\hat{\gamma}_1^f = [\angle(r_{1,1} \bar{s}_{1,k}^*), \dots, \angle(r_{D,1} \bar{s}_{D,k}^*)]^T, \quad (48)$$

$$\mathbf{M}_1^f = \text{diag}(\bar{\sigma}_{1,k}^2, \dots, \bar{\sigma}_{D,k}^2). \quad (49)$$

Using (43) and the Gaussian approximation of $p(\gamma_k|\mathbf{r})$, $P_u(s_{i,k})$ can be described in closed form as

$$\begin{aligned} P_u(s_{i,k}) &\propto \int_{\mathbb{R}^D} p(r_{i,k}|s_{i,k}, \gamma_{i,k}) \frac{p(\gamma_k|\mathbf{r})}{p(r_{i,k}|\gamma_{i,k})} d\gamma_k \\ &= \int_{\mathbb{R}} \frac{\mathcal{N}_{r_{i,k}}(s_{i,k} e^{j\gamma_{i,k}}, \sigma_i^2)}{p(r_{i,k}|\gamma_{i,k})} \left[\int_{\mathbb{R}^{D-1}} p(\gamma_k|\mathbf{r}) d\bar{\gamma}_{i,k} \right] d\gamma_{i,k} \quad (50) \\ &\approx \int_{\mathbb{R}} \frac{\mathcal{N}_{r_{i,k}}(s_{i,k} e^{j\gamma_{i,k}}, \sigma_i^2)}{\mathcal{N}_{r_{i,k}}(\bar{s}_{i,k} e^{j\gamma_{i,k}}, \bar{\sigma}_{i,k}^2)} \\ &\quad \cdot \left[\int_{\mathbb{R}^{D-1}} \mathcal{N}_{\gamma_k}(\hat{\gamma}_k^s, \mathbf{M}_k^s) d\bar{\gamma}_{i,k} \right] d\gamma_{i,k} \quad (51) \end{aligned}$$

$$= \int_{\mathbb{R}} \frac{\mathcal{N}_{r_{i,k}}(s_{i,k} e^{j\gamma_{i,k}}, \sigma_i^2)}{\mathcal{N}_{r_{i,k}}(\bar{s}_{i,k} e^{j\gamma_{i,k}}, \bar{\sigma}_{i,k}^2)} \mathcal{N}_{\gamma_{i,k}}(\hat{\gamma}_{i,k}^s, M_{i,k}^s) d\gamma_{i,k} \quad (52)$$

$$\propto e^{-\frac{|s_{i,k}|^2}{2}} \int_{\mathbb{R}} \exp\left(\Re\left\{\left(\frac{r_{i,k} s_{i,k}^*}{\sigma_i^2} - \frac{r_{i,k} \bar{s}_{i,k}^*}{\bar{\sigma}_{i,k}^2}\right) e^{-j\gamma_{i,k}}\right\}\right) d\gamma_{i,k} \quad (53)$$

$$\approx e^{-\frac{|s_{i,k}|^2}{2}} \int_{\hat{\gamma}_{i,k}^s - \pi}^{\hat{\gamma}_{i,k}^s + \pi} \exp\left(\Re\left\{\left(\frac{r_{i,k} s_{i,k}^*}{\sigma_i^2} - \frac{r_{i,k} \bar{s}_{i,k}^*}{\bar{\sigma}_{i,k}^2}\right) e^{-j\gamma_{i,k}}\right\}\right) \mathcal{T}_{\gamma_{i,k}}\left(\frac{e^{j\hat{\gamma}_{i,k}^s}}{M_{i,k}^s}\right) d\gamma_{i,k} \quad (54)$$

$$\propto e^{-\frac{|s_{i,k}|^2}{2}} \int_{\hat{\gamma}_{i,k}^s - \pi}^{\hat{\gamma}_{i,k}^s + \pi} \exp(\Re\{\xi_{i,k} e^{-j\gamma_{i,k}}\}) d\gamma_{i,k} \quad (55)$$

$$\propto e^{-\frac{|s_{i,k}|^2}{2}} I_0(|\xi_{i,k}|) \int_{\hat{\gamma}_{i,k}^s - \pi}^{\hat{\gamma}_{i,k}^s + \pi} \mathcal{T}_{\gamma_{i,k}}(\xi_{i,k}) d\gamma_{i,k} \quad (56)$$

$$= e^{-\frac{|s_{i,k}|^2}{2}} I_0(|\xi_{i,k}|) \quad (57)$$

$$\approx \frac{1}{\sqrt{|\xi_{i,k}|}} \exp\left(|\xi_{i,k}| - \frac{|s_{i,k}|^2}{2}\right), \quad (58)$$

with

$$\xi_{i,k} \triangleq \frac{e^{j\hat{\gamma}_{i,k}^s}}{M_{i,k}^s} + \frac{r_{i,k} s_{i,k}^*}{\sigma_i^2} - \frac{r_{i,k} \bar{s}_{i,k}^*}{\bar{\sigma}_{i,k}^2}, \quad (59)$$

where $\bar{\gamma}_{i,k}$ contains all elements of γ_k except $\gamma_{i,k}$, (52) exploits the fact that a multivariate Gaussian is trivially marginalized [30, Ch. 8], and (54) uses the approximation $\mathcal{N}_z(\mu, \sigma^2) \approx \mathcal{T}_z(e^{j\mu}/\sigma^2)$, which is accurate for small σ^2 [14]. Moreover, $\hat{\gamma}_{i,k}^s$ and $M_{i,k}^s$ denote the i th element of $\hat{\gamma}_k^s$ and the i th element on the diagonal line of \mathbf{M}_k^s , respectively. Note that the expression in (58) only describes $P_u(s_{i,k})$ up to a constant, and therefore needs to be normalized. It is also numerically troublesome, and thus, the logarithm of (58) can be computed instead, yielding

$$\begin{aligned} \ln P_u(s_{i,k}) &\propto \ln \left[\int_{\mathbb{R}^D} p(r_{i,k}|s_{i,k}, \gamma_{i,k}) \frac{p(\gamma_k|\mathbf{r})}{p(r_{i,k}|\gamma_{i,k})} d\gamma_k \right] \\ &\approx |\xi_{i,k}| - \frac{|s_{i,k}|^2}{2\sigma_i^2} - \frac{1}{2} \ln |\xi_{i,k}| \quad (60) \end{aligned}$$

$$\triangleq f_{i,k}(s_{i,k}). \quad (61)$$

Finally, $P_u(s_{i,k})$ is computed from $f(s_{i,k})$ as

$$P_u(s_{i,k}) = \exp(f_{i,k}(s_{i,k}) - C_{i,k}), \quad (62)$$

where

$$C_{i,k} = f_{i,k}^{\max} - \log \sum_{s_{i,k} \in \mathcal{X}} e^{f_{i,k}(s_{i,k}) - f_{i,k}^{\max}} \quad (63)$$

and $f_{i,k}^{\max} \triangleq \max_{s_{i,k} \in \mathcal{X}} f_{i,k}(s_{i,k})$. This algorithm will from now on be referred to as FG/SPA Phase-Noise Compensation (FG-PNC) and is summarized in Algorithm 2, where the sets of $P_d(s_{i,k})$ and $P_u(s_{i,k})$ for all (i,k) are denoted with $\{P_d(s_{i,k})\}$ and $\{P_u(s_{i,k})\}$, resp.

C. VB-Based Algorithm

We now apply VB inference to the marginalization problem in (4), in which $p(\mathbf{b}, \gamma|\mathbf{r}) = \chi[\mathbf{s} = f(\mathbf{b})]p(\mathbf{s}, \gamma|\mathbf{r})$ in (4) is approximated with a family of factorized distributions, $q_S(\mathbf{s})q_\Gamma(\gamma)$. The objective is then to minimize the KL divergence [32] between $q_S(\mathbf{s})q_\Gamma(\gamma)$ and $p(\mathbf{b}, \gamma|\mathbf{r})$, i.e.,

$$\min_{q_S(\mathbf{s}), q_\Gamma(\gamma)} D(q_S(\mathbf{s})q_\Gamma(\gamma) || p(\mathbf{b}, \gamma|\mathbf{r})). \quad (64)$$

Algorithm 2 FG-PNC**Input:** $\mathbf{r}, \{P_d(s_{i,k})\}, D, N, \mathbf{Q}, \sigma^2, \mathcal{X}$ **Output:** $\{P_u(s_{i,k})\}$

```

1: for all  $(i, k)$  do
2:    $\bar{s}_{i,k} = \sum_{s_{i,k} \in \mathcal{X}} P_d(s_{i,k})$ 
3:    $\bar{\sigma}_{i,k}^2 = \sigma_i^2 + \sum_{s_{i,k} \in \mathcal{X}} |s_{i,k} - \bar{s}_{i,k}|^2 P_d(s_{i,k})$ 
4: end for
5: Compute  $\{(\hat{\gamma}_k^s, \mathbf{M}_k^s)\}$  with Alg. 1 using (46)–(49)
6: for all  $(i, k)$  do
7:   for all  $s_{i,k} \in \mathcal{X}$  do
8:      $\xi_{i,k} = \frac{e^{j\hat{\gamma}_{i,k}^s}}{M_{i,k}^s} + \frac{r_{i,k} s_{i,k}^*}{\sigma_i^2} - \frac{r_{i,k} \bar{s}_{i,k}^*}{\bar{\sigma}_{i,k}^2}$ 
9:      $f_{i,k}(s_{i,k}) = |\xi_{i,k}| - \frac{|s_{i,k}|^2}{2\sigma_i^2} - \frac{1}{2} \ln |\xi_{i,k}|$ 
10:   end for
11:    $f_{i,k}^{\max} = \max_{s_{i,k} \in \mathcal{X}} f_{i,k}(s_{i,k})$ 
12:    $C_{i,k} = f_{i,k}^{\max} - \sum_{s_{i,k} \in \mathcal{X}} e^{f_{i,k}(s_{i,k}) - f_{i,k}^{\max}}$ 
13:   for all  $s_{i,k} \in \mathcal{X}$  do
14:      $P_u(s_{i,k}) = \exp(f_{i,k}(s_{i,k}) - C_{i,k})$ 
15:   end for
16: end for

```

This minimization is carried out by iteratively updating $q_S(\mathbf{s})$ and $q_\Gamma(\gamma)$, and it can be shown that the update equations at the l th iteration are expressed as

$$q_\Gamma^{(l)}(\gamma) \propto p(\gamma) \exp\left(\mathbb{E}_{q_S^{(l-1)}}[\log p(\mathbf{r}|\mathbf{S}, \gamma)]\right), \quad (65)$$

$$q_S^{(l)}(\mathbf{s}) \propto \chi[\mathbf{s} = f(\mathbf{b})] \exp\left(\mathbb{E}_{q_\Gamma^{(l)}}[\log p(\mathbf{r}|\mathbf{S}, \Gamma)]\right), \quad (66)$$

for $l = 1, \dots, T$, where \propto denotes proportionality w.r.t. γ and \mathbf{s} , and $p(\mathbf{r}|\mathbf{s}, \gamma)$ is the likelihood function of \mathbf{s} . For more details on this framework and on the results in (65) and (66), we refer the reader to [17]. The rest of the subsection describes the computation of $q_\Gamma^{(l)}(\gamma)$ and $q_S^{(l)}(\mathbf{s})$ for one iteration, and therefore, the superscript indicating the iteration number will be skipped hereafter for notational convenience.

The likelihood function is a multivariate Gaussian PDF that can be factorized into a product of univariate Gaussian PDFs, since all received samples are statistically independent when γ is given. Hence,

$$q_\Gamma(\gamma) \propto p(\gamma) \prod_{(i,k)} \exp\left(-\frac{1}{2\sigma_i^2} \mathbb{E}_{q_{S_{i,k}}} \left[|r_{i,k} - S_{i,k} e^{j\gamma_{i,k}}|^2 \right]\right) \quad (67)$$

for $i = 1, \dots, D$ and $k = 1, \dots, N$, and

$$\begin{aligned} & \mathbb{E}_{q_{S_{i,k}}} \left[|r_{i,k} - S_{i,k} e^{j\gamma_{i,k}}|^2 \right] \\ &= \left| r_{i,k} - \mathbb{E}_{q_{S_{i,k}}} [S_{i,k}] e^{j\gamma_{i,k}} \right|^2 + \text{Var}[S_{i,k}] \end{aligned} \quad (68)$$

$$= \left| r_{i,k} - \bar{s}_{i,k} e^{j\gamma_{i,k}} \right|^2 + \text{Var}[S_{i,k}], \quad (69)$$

where

$$\bar{s}_{i,k} \triangleq \mathbb{E}_{q_{S_{i,k}}} [S_{i,k}] = \sum_{s_{i,k} \in \mathcal{X}} s_{i,k} q_{S_{i,k}}(s_{i,k}), \quad (70)$$

and (68) uses the fact that $\mathbb{E}[|\cdot|^2] = \text{Var}[\cdot] + |\mathbb{E}[\cdot]|^2$, and $\text{Var}[S_{i,k}] = \sum_{s_{i,k} \in \mathcal{X}} |s_{i,k} - \bar{s}_{i,k}|^2 q_{S_{i,k}}(s_{i,k})$. Analogously to

the FG/SPA based algorithm, $\bar{s}_{i,k} = s_{i,k}$ for pilot symbols during each iteration, and for information symbols, $\bar{s}_{i,k}$ is initialized as 0. Thus,

$$\begin{aligned} q_\Gamma(\gamma) & \propto p(\gamma) \prod_{(i,k)} \exp\left(-\frac{1}{2\sigma_i^2} \left(|r_{i,k} - \bar{s}_{i,k} e^{j\gamma_{i,k}}|^2 + \text{Var}[S_{i,k}] \right)\right) \\ & \propto p(\gamma) \prod_{(i,k)} \exp\left(-\frac{1}{2\sigma_i^2} |r_{i,k} - \bar{s}_{i,k} e^{j\gamma_{i,k}}|^2\right). \end{aligned} \quad (71)$$

Moreover,

$$\begin{aligned} q_S(\mathbf{s}) & \propto \chi[\mathbf{s} = f(\mathbf{b})] \\ & \cdot \prod_{i,k} \exp\left(-\frac{1}{2\sigma_i^2} \mathbb{E}_{q_{\Gamma_{i,k}}} \left[|r_{i,k} - s_{i,k} e^{j\Gamma_{i,k}}|^2 \right]\right) \end{aligned} \quad (72)$$

for $i = 1, \dots, D$ and $k = 1, \dots, N$, and

$$\begin{aligned} & \mathbb{E}_{q_{\Gamma_{i,k}}} \left[|r_{i,k} - s_{i,k} e^{j\Gamma_{i,k}}|^2 \right] \\ &= |r_{i,k}|^2 - 2\Re\{r_{i,k}(s_{i,k}\alpha_{i,k})^*\} + |s_{i,k}|^2, \end{aligned} \quad (73)$$

where $\alpha_{i,k} \triangleq \mathbb{E}_{q_{\Gamma_{i,k}}} [e^{j\Gamma_{i,k}}]$. Therefore,

$$\begin{aligned} q_S(\mathbf{s}) & \propto \chi[\mathbf{s} = f(\mathbf{b})] \prod_{(i,k)} \exp\left(\frac{\Re\{r_{i,k}(s_{i,k}\alpha_{i,k})^*\}}{\sigma_i^2} - \frac{|s_{i,k}|^2}{2\sigma_i^2}\right). \end{aligned} \quad (74)$$

From (67), it can be seen that $q_\Gamma(\gamma)$ relies on $q_{S_{i,k}}(s_{i,k})$, the marginals of $q_S(\mathbf{s})$. Likewise, (72) shows that $q_S(\mathbf{s})$ relies on $q_{\Gamma_{i,k}}(\gamma_{i,k})$, the marginals of $q_\Gamma(\gamma)$. Thus, computing (65) and (66) involves the marginalizations of $q_\Gamma(\gamma)$ and $q_S(\mathbf{s})$.

1) *Marginalization of $q_\Gamma(\gamma)$* : The distribution $q_\Gamma(\gamma)$ is approximated as a multivariate Gaussian distribution, and the marginals $q_{\Gamma_{i,k}}(\gamma_{i,k})$ can be estimated in the same fashion as $p(\gamma_k|\mathbf{r})$ in (39), i.e., with the EKF and RTSS. Thus, the parameters $\hat{\gamma}_k^s$ and \mathbf{M}_k^s are computed with (24)–(26) and (30)–(32), and they represent the mean vector and covariance matrix of the Gaussian approximation of $q_{\Gamma_k}(\gamma_k)$, i.e.,

$$q_{\Gamma_k}(\gamma_k) \approx \mathcal{N}_{\gamma_k}(\hat{\gamma}_k^s, \mathbf{M}_k^s). \quad (75)$$

Due to (71), \mathbf{S}_k in (25) and each component of \mathbf{h}_k in (26) are computed as

$$\mathbf{S}_k = \text{diag}\left(\frac{|\bar{s}_{1,k}|^2}{\sigma_1^2}, \dots, \frac{|\bar{s}_{D,k}|^2}{\sigma_D^2}\right), \quad (76)$$

$$h_{i,k} = \frac{1}{\sigma_i^2} \Im\left\{r_{i,k}(\bar{s}_{i,k})^* e^{-j\hat{\gamma}_{i,k}^f}\right\}, \quad (77)$$

and the EKF equations are initialized with

$$\hat{\gamma}_1^f = [\angle(r_{1,1}(\bar{s}_{1,k})^*), \dots, \angle(r_{D,1}(\bar{s}_{D,k})^*)]^T, \quad (78)$$

$$\mathbf{M}_1^f = \text{diag}(\sigma_1^2, \dots, \sigma_D^2). \quad (79)$$

Further marginalizing $q_{\Gamma_k}(\gamma_k)$ to obtain $q_{\Gamma_{i,k}}(\gamma_{i,k})$ is trivial under the assumption that $q_{\Gamma_k}(\gamma_k)$ is a Gaussian distribution, i.e., it is given by

$$q_{\Gamma_{i,k}}(\gamma_{i,k}) = \mathcal{N}_{\gamma_{i,k}}(\hat{\gamma}_{i,k}^s, M_{i,k}^s). \quad (80)$$

2) *Marginalization of $q_S(\mathbf{s})$* : As was shown before, the function $q_S(\mathbf{s})$ can be expressed as

$$\begin{aligned} q_S(\mathbf{s}) &\propto \chi[\mathbf{s} = f(\mathbf{b})] \prod_{(i,k)} \exp\left(\frac{\Re\{r_{i,k}(s_{i,k}\alpha_{i,k})^*\}}{\sigma_i^2} - \frac{|s_{i,k}|^2}{2\sigma_i^2}\right) \\ &\propto \chi[\mathbf{s} = f(\mathbf{b})] \prod_{(i,k)} g_{i,k}(s_{i,k}), \end{aligned} \quad (81)$$

where $g_{i,k}(s_{i,k})$ corresponds to the likelihood function of $s_{i,k}$ from a virtual memoryless phase-noise compensated channel, analogously to $P_u(s_{i,k})$ in (58). Moreover, given that $q_{\Gamma}(\gamma)$ is approximated as a Gaussian distribution,

$$\begin{aligned} \alpha_{i,k} &= \mathbb{E}_{q_{\Gamma_{i,k}}} [e^{j\Gamma_{i,k}}] \\ &\approx \int_{-\infty}^{\infty} e^{j\gamma_{i,k}} \mathcal{N}_{\gamma_{i,k}}(\hat{\gamma}_{i,k}^s, M_{i,k}^s) d\gamma_{i,k} \\ &= \frac{1}{\sqrt{2\pi M_{i,k}^s}} \int_{-\infty}^{\infty} \exp\left(j\gamma_{i,k} - \frac{1}{2M_{i,k}^s}(\gamma_{i,k} - \hat{\gamma}_{i,k}^s)^2\right) d\gamma_{i,k} \\ &= \exp\left(j\hat{\gamma}_{i,k}^s - \frac{M_{i,k}^s}{2}\right) \frac{1}{\sqrt{2\pi M_{i,k}^s}} \\ &\quad \cdot \int_{-\infty}^{\infty} \exp\left(-\left(\frac{\gamma_{i,k} - \hat{\gamma}_{i,k}^s}{\sqrt{2M_{i,k}^s}} - j\sqrt{\frac{M_{i,k}^s}{2}}\right)^2\right) d\gamma_{i,k} \\ &= \exp\left(j\hat{\gamma}_{i,k}^s - \frac{M_{i,k}^s}{2}\right) \frac{1}{\sqrt{\pi}} \int_{-\infty}^{\infty} \exp(-u^2) du \\ &= \exp\left(j\hat{\gamma}_{i,k}^s - \frac{M_{i,k}^s}{2}\right), \end{aligned} \quad (82)$$

where (82) is obtained through change of variables, i.e.,

$$u = \frac{\gamma_{i,k} - \hat{\gamma}_{i,k}^s}{\sqrt{2M_{i,k}^s}} - j\sqrt{\frac{M_{i,k}^s}{2}}, \quad (84)$$

and (83) exploits the fact that the integral in (82) is the Euler–Poisson integral, which evaluates to $\sqrt{\pi}$.

To obtain $q_{S_{i,k}}(s_{i,k})$, which is analogous to the message $P_u(s_{i,k})$ in (39) and is used to compute $q_{\Gamma}(\gamma)$ in (67) during a consecutive iteration, $q_S(\mathbf{s})$ is marginalized over all symbols except $s_{i,k}$. The marginalization of $q_S(\mathbf{s})$ is performed in the decoder, where the function $g_{i,k}(s_{i,k})$ in (81) is converted to bit-wise LLRs that are fed to decoder. The decoder then either outputs the detected information bits or a *posteriori* LLRs of the coded bits, which are converted to $q_{S_{i,k}}(s_{i,k})$. Note that for uncoded transmission, this marginalization is trivial since the transmitted symbols are independent of each other. Thus,

$$q_{S_{i,k}}(s_{i,k}) \propto P(s_{i,k})g_{i,k}(s_{i,k}), \quad (85)$$

where $P(s_{i,k})$ is a uniform PMF for information symbols and a degenerate distribution for pilot symbols, i.e., equal to 1 if $s_{i,k}$ is equal to the pilot and 0 otherwise. This algorithm will be referred to as VB Phase-Noise Compensation (VB-PNC) and is summarized in Algorithm 3, where $\{g_{i,k}(s_{i,k})\}$ denotes the set of $g_{i,k}(s_{i,k})$ for all (i,k) .

Algorithm 3 VB-PNC

Input: \mathbf{r} , $\{q_{S_{i,k}}^{(l-1)}(s_{i,k})\}$, D , N , \mathbf{Q} , σ^2 , \mathcal{X}

Output: $\{g_{i,k}^{(l)}(s_{i,k})\}$

```

1: for all  $(i,k)$  do
2:    $\bar{s}_{i,k} = \sum_{s_{i,k} \in \mathcal{X}} q_{S_{i,k}}^{(l-1)}(s_{i,k})$ 
3: end for
4: Compute  $\{(\gamma_k^s, \mathbf{M}_k^s)\}$  with Alg. 1 using (76)–(79)
5: for all  $(i,k)$  do
6:    $\alpha_{i,k} = \exp(j\hat{\gamma}_{i,k}^s - M_{i,k}^s/2)$ 
7:   for all  $s_{i,k} \in \mathcal{X}$  do
8:      $g_{i,k}^{\text{tmp}}(s_{i,k}) = \exp\left(\frac{\Re\{r_{i,k}(s_{i,k}\alpha_{i,k})^*\}}{\sigma_i^2} - \frac{|s_{i,k}|^2}{2\sigma_i^2}\right)$ 
9:   end for
10:   $K = \sum_{s_{i,k} \in \mathcal{X}} g_{i,k}^{\text{tmp}}(s_{i,k})$ 
11:  for all  $s_{i,k} \in \mathcal{X}$  do
12:     $g_{i,k}^{(l)}(s_{i,k}) = g_{i,k}^{\text{tmp}}(s_{i,k})/K$ 
13:  end for
14: end for

```

D. Connection to Decoder

As detailed in the previous subsections, the inputs and outputs to FG-PNC and VB-PNC are in the form of symbol PMFs. However, iterative decoders for LDPC codes and turbo codes are typically implemented in the logarithm domain [28, Ch. 5], and thus, have bit-wise LLRs as inputs and outputs.

The computation of bit-wise input LLRs from the *a posteriori* symbol PMFs is done as follows. For each transmitted symbol $s_{i,k}$, the LLR for the j th bit in the binary labeling of the constellation points is computed from the *a posteriori* PMF of $s_{i,k}$ as

$$\begin{aligned} L(b_i) &\triangleq \log\left(\frac{P(r_{i,k}|b_{i,k}^j = 0)}{P(r_{i,k}|b_{i,k}^j = 1)}\right) \\ &= \log\left(\frac{\sum_{s_{i,k} \in \mathcal{B}_0} P(r_{i,k}|s_{i,k})}{\sum_{s_{i,k} \in \mathcal{B}_1} P(r_{i,k}|s_{i,k})}\right), \end{aligned} \quad (86)$$

for $j = 1, \dots, R_m$, where $R_m \triangleq \log_2 |\mathcal{X}|$ and \mathcal{B}_ν is the set of constellation points that have the j th bit in the binary labeling as $\nu \in \{0, 1\}$. In relation to the proposed algorithms, $P(r_{i,k}|s_{i,k})$ corresponds to $P_u(s_{i,k})$ for FG-PNC and $g_{i,k}(s_{i,k})$ for VB-PNC.

The output LLRs from the decoder are defined as

$$L(b_{i,k}^j|\mathbf{r}) \triangleq \log\left(\frac{P(b_{i,k}^j = 0|\mathbf{r})}{P(b_{i,k}^j = 1|\mathbf{r})}\right), \quad (87)$$

and noting that $P(b_{i,k}^j = 1|\mathbf{r}) = 1 - P(b_{i,k}^j = 0|\mathbf{r})$, rearranging (87) gives

$$P(b_{i,k}^j = 0|\mathbf{r}) = \frac{e^{L(b_{i,k}^j|\mathbf{r})}}{1 + e^{L(b_{i,k}^j|\mathbf{r})}} \quad (88)$$

With a slight abuse of notation, denote the extrinsic information about $s_{i,k}$ being a constellation point with binary labeling

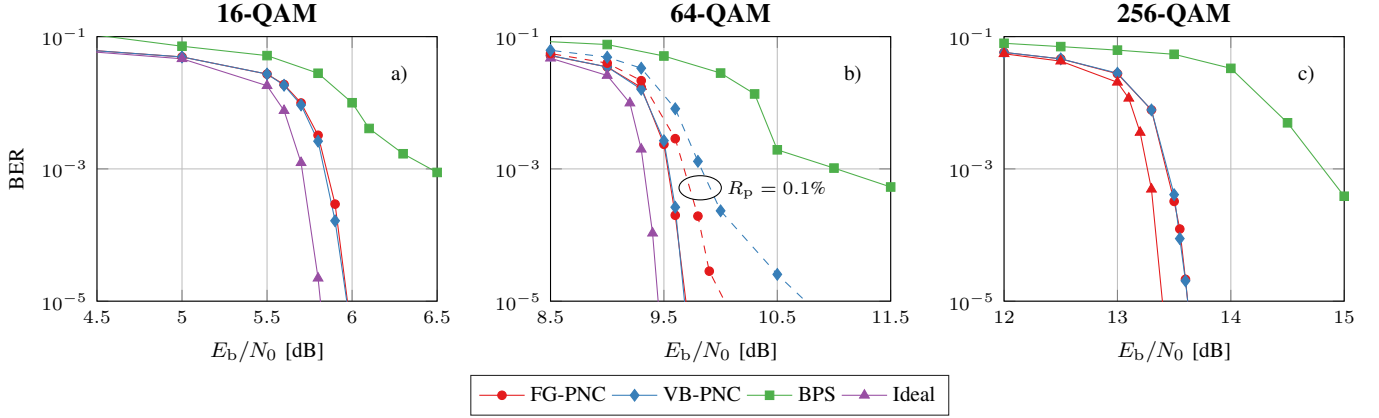


Fig. 2. BER versus SNR per information bit for 16-QAM and 1MHz laser linewidth (left), 64-QAM and 1MHz laser linewidth (middle), and 256-QAM and 100kHz laser linewidth (right), assuming a symbol rate of 20 GBaud. The dashed lines in the middle plot correspond to $R_p = 0.1\%$.

$(\nu_1, \dots, \nu_{R_m}) \in \{0, 1\}^{R_m}$ as $P_e(s_{i,k} = (\nu_1, \dots, \nu_{R_m}))$, which is then computed as

$$P_e(s_{i,k} = (\nu_1, \dots, \nu_{R_m})) = \prod_{j=1}^{R_m} P(b_{i,k}^j = \nu_j | \mathbf{r}). \quad (89)$$

Here, $P_e(s_{i,k})$ corresponds to $P_d(s_{i,k})$ for FG-PNC and $q_{S_{i,k}}(s_{i,k})$ for VB-PNC.

IV. SIMULATION RESULTS

In this section, the proposed algorithms are assessed in terms of phase-noise tolerance through Monte Carlo simulations, and their performance is compared to separate channel processing using BPS. Coded transmission over 20 channels of 16-QAM, 64-QAM, and 256-QAM is considered. A rate-4/5 LDPC code from the DVB-S.2 standard is utilized to encode data independently for each channel, yielding a codeword of length 64800 bits per channel. The pilot symbols are arranged in a wrapped diagonal fashion, which is shown in [33] to perform well for multichannel transmission with correlated phase noise. Furthermore, the variance of the AWGN is kept identical for all channels and the phase noise is partly correlated across the channels. To realize the phase-noise correlation, the covariance matrix of $\Delta\gamma_k$ in (2) is constructed such that elements on the diagonal are equal to $\sigma_\theta^2 + \sigma_\delta^2$, with $\sigma_\delta^2 = \sigma_\theta^2/1000$, while all other elements are equal to σ_δ^2 , where $\sigma_\theta^2 = 2\pi\Delta\nu T_s$ is the laser phase noise variance and is a function of the laser linewidth, $\Delta\nu$, and the symbol duration, T_s . This corresponds to a single dominant laser phase noise component that is common to all channels, in addition to slower phase drifts that are independent between channels. The laser linewidth and symbol duration product, $\Delta\nu T_s$, is fixed at $5 \cdot 10^{-5}$ for 16-QAM and 64-QAM, and $5 \cdot 10^{-6}$ for 256-QAM. Assuming a 20 GBaud symbol rate, this corresponds to a laser linewidths of 1 MHz and 100kHz.

The scheduling for the proposed algorithms is as follows. A total of 6 outer iterations between the phase-noise compensation and decoding are performed. The decoder state is between each outer iteration. For the first 5 outer iterations, 1 decoding iteration is performed in the LDPC decoder per outer iteration. In the last outer iteration, the decoder is run

for 20 decoding iterations and the information bits are detected afterwards, yielding a total of 25 decoding iterations.

When performing phase-noise compensation using BPS, 32 test phases are used for transmission of 16-QAM, whereas 64 test phases are used for 64-QAM and 256-QAM. A filter half width between 35 and 45 is used. No differential encoding is used, but instead, the initial value of the phase noise is assumed to be known. Moreover, no outer iterations are needed since BPS does not take advantage of the symbol statistics. Thus, following BPS, the decoder directly performs 25 decoding iterations, after which the information bits are detected.

BER results are obtained by counting a minimum of 100 frame errors. The BER is computed as a function of signal-to-noise ratio (SNR) per information bit,

$$\frac{E_b}{N_0} \triangleq \frac{E_s}{2\sigma^2 R_c R_m (1 - R_p)}, \quad (90)$$

where σ^2 is the AWGN variance, and R_p , R_c , and R_m are the pilot rate, code rate, and bits per symbol, resp. Furthermore, the BER performance of coded transmission over the AWGN channel in the absence of pilot symbols is included as an ideal performance of perfect phase-noise compensation.

Fig. 2 a), b), and c) show results for coded transmission of 16-QAM and 64-QAM, and 256-QAM, resp., using 1% pilot rate for the proposed algorithms, FG-PNC and VB-PNC. In all cases, the proposed algorithms perform almost identically and greatly outperform the traditional approach of individual phase-noise compensation on each channel with BPS. Compared to the ideal performance, the proposed algorithms result in roughly 0.1 dB, 0.2 dB, and 0.2 dB SNR penalty for 16-QAM, 64-QAM, and 256-QAM resp. Moreover, Fig. 2 b) includes results for FG-PNC and VB-PNC using 0.1% pilot rate, shown in the dashed curves. In this case, FG-PNC demonstrates superior performance to VB-PNC.

The strong performance of the proposed algorithms can be attributed to the following: Due to the partial correlation in the phase noise, the pilot symbol distribution allows for a more effective use of the pilots in multichannel processing compared to single-channel processing. Furthermore, the algorithms make use of the phase-noise statistics when computing

the *a posteriori* symbol PMFs, which has been shown to be a superior strategy than separating the phase-noise compensation and data detection [34]. Finally, the iterative cooperation with the decoder improves the phase-noise compensation performance, and thus, the resulting BER. As expected, however, the amount of performance improvement diminishes with increasing number of outer iterations.

V. CONCLUSIONS

The problem of compensating for coded multichannel optical transmission in the presence of correlated phase noise was investigated. A multichannel phase-noise model was introduced and used in conjunction with two frameworks to approximate the MAP detector. The resulting pilot-aided algorithms exploit the phase-noise correlation across channels, allowing for a more effective compensation than what can be achieved through single-channel processing. The algorithms were assessed in terms of phase-noise tolerance for different modulation formats, amounts of phase noise, and pilot rates. Through Monte Carlo simulations, it was shown that the proposed algorithms outperform conventional phase-noise compensation by a wide margin, giving rise to an insignificant SNR penalty of 0.1 dB, 0.2 dB, and 0.2 dB for 16-QAM, 64-QAM, and 256-QAM, resp., with respect to perfect compensation in the presence of strong phase noise.

REFERENCES

- [1] E. Ip, A. P. T. Lau, D. J. F. Barros, and J. M. Kahn, "Coherent detection in optical fiber systems," *Opt. Exp.*, vol. 16, no. 2, pp. 753–791, Jan. 2008.
- [2] M. Karlsson and E. Agrell, "Multidimensional modulation and coding in optical transport," *J. Lightwave Technol.*, vol. 35, no. 4, pp. 876–884, Feb. 2017.
- [3] A. J. Viterbi, "Nonlinear estimation of PSK-modulated carrier phase with application to burst digital transmission," *IEEE Trans. Inf. Theory*, vol. 29, no. 4, pp. 543–551, Jul. 1983.
- [4] T. Pfau, S. Hoffmann, and R. Noé, "Hardware-efficient coherent digital receiver concept with feedforward carrier recovery for M-QAM constellations," *J. Lightw. Technol.*, vol. 27, no. 8, pp. 989–999, Apr. 2009.
- [5] E. Ip and J. M. Kahn, "Feedforward carrier recovery for coherent optical communications," *J. Lightw. Technol.*, vol. 25, no. 9, pp. 2675–2692, Sep. 2007.
- [6] J. M. Kahn and D. A. B. Miller, "Communications expands its space," *Nature Photonics*, vol. 11, no. 1, pp. 5–8, Jan. 2017.
- [7] M. D. Feuer, L. E. Nelson, X. Zhou, S. L. Woodward, R. Isaac, B. Zhu, T. F. Taunay, M. Fishteyn, J. M. Fini, and M. F. Yan, "Joint digital signal processing receivers for spatial superchannels," *IEEE Photonics Technol. Lett.*, vol. 24, no. 21, pp. 1957–1960, Nov. 2012.
- [8] A. F. Alfredsson *et al.*, "Phase-noise compensation for spatial-division multiplexed transmission," in *Proc. Opt. Fiber Commun. Conf. Optical Society of America*, Mar. 2017, paper Th4C.7.
- [9] B. J. Puttnam, R. S. Luis, J. M. D. Mendinueta, J. Sakaguchi, W. Klaus, Y. Awaji, N. Wada, A. Kanno, and T. Kawanishi, "Long distance transmission in a multi-core fiber with self-homodyne detection," in *Proc. Opt. Fiber Commun. Conf.*, Mar. 2015, paper Th1D.5.
- [10] R. S. Luis *et al.*, "Comparing inter-core skew fluctuations in multi-core and single-core fibers," in *Proc. Lasers and Electro-Opt.*, May 2015, paper SM2L.5.
- [11] L. Lundberg, M. Mazur, A. Lorences-Riesgo, M. Karlsson, and P. A. Andrekson, "Joint carrier recovery for DSP complexity reduction in frequency comb-based superchannel transceivers," in *Proc. European Conf. Opt. Commun.*, Sep. 2017, paper Th.1.D.3.
- [12] D. V. Souto, B. E. Olsson, C. Larsson, and D. A. A. Mello, "Joint-polarization and joint-subchannel carrier phase estimation for 16-QAM optical systems," *J. Lightwave Technol.*, vol. 30, no. 20, pp. 3185–3191, Oct. 2012.
- [13] R. G. H. van Uden, C. M. Okonkwo, V. A. J. M. Sleiffer, M. Kushnerov, H. de Waardt, and A. M. J. Koonen, "Single DPLL joint carrier phase compensation for few-mode fiber transmission," *IEEE Photonics Technol. Lett.*, vol. 25, no. 14, pp. 1381–1384, Jul. 2013.
- [14] G. Colavolpe, A. Barbieri, and G. Caire, "Algorithms for iterative decoding in the presence of strong phase noise," *IEEE J. Sel. Areas Commun.*, vol. 23, no. 9, pp. 1748–1757, Sep. 2005.
- [15] N. Noels, J. Bhatti, H. Bruneel, and M. Moeneclaey, "Block-processing soft-input soft-output demodulator for coded PSK using DCT-based phase noise estimation," *IEEE Trans. Commun.*, vol. 62, no. 8, pp. 2939–2950, Aug. 2014.
- [16] J. Dauwels and H. A. Loeliger, "Joint decoding and phase estimation: an exercise in factor graphs," in *Proc. IEEE International Symposium on Inf. Theory*, Jun. 2003.
- [17] M. Nissilä and S. Pasupathy, "Adaptive iterative detectors for phase-uncertain channels via variational bounding," *IEEE Trans. Commun.*, vol. 57, no. 3, pp. 716–725, Mar. 2009.
- [18] N. Noels, V. Lottici, A. Dejonghe, H. Steendam, M. Moeneclaey, M. Luise, and L. Vandendorpe, "A theoretical framework for soft-information-based synchronization in iterative (turbo) receivers," *EURASIP J. Wirel. Commun. Netw.*, vol. 2005, no. 2, pp. 117–129, Apr. 2005.
- [19] T. S. Shehata and M. El-Tanany, "Joint iterative detection and phase noise estimation algorithms using kalman filtering," in *Canadian Workshop on Inf. Theory*, May 2009, pp. 165–168.
- [20] T. C. W. Schenk, X.-J. Tao, P. F. M. Smulders, and E. R. Fledderus, "Influence and suppression of phase noise in multi-antenna OFDM," in *Proc. Vehicular Technol. Conf.*, vol. 2, Sep. 2004, pp. 1443–1447.
- [21] R. Krishnan, G. Colavolpe, A. Graell i Amat, and T. Eriksson, "Algorithms for joint phase estimation and decoding for MIMO systems in the presence of phase noise and quasi-static fading channels," *IEEE Trans. Signal Process.*, vol. 63, no. 13, pp. 3360–3375, Jul. 2015.
- [22] A. O. Isikman, H. Mehrpouyan, A. A. Nasir, A. G. Amat, and R. A. Kennedy, "Joint phase noise estimation and data detection in coded multi-input–multi-output systems," *IET Commun.*, vol. 8, no. 7, pp. 981–989, May 2014.
- [23] H. Mehrpouyan, A. A. Nasir, S. D. Blostein, T. Eriksson, G. K. Karagiannidis, and T. Svensson, "Joint estimation of channel and oscillator phase noise in MIMO systems," *IEEE Trans. on Signal Process.*, vol. 60, no. 9, pp. 4790–4807, Sep. 2012.
- [24] F. R. Kschischang, B. J. Frey, and H.-A. Loeliger, "Factor graphs and the sum-product algorithm," *IEEE Trans. Inf. Theory*, vol. 47, no. 2, pp. 498–519, Feb. 2001.
- [25] M. J. Beal, "Variational algorithms for approximate bayesian inference," Ph.D. dissertation, University College London, 2003.
- [26] J. van Weerdenburg, R. Ryf, J. C. Alvarado-Zacarias, R. A. Alvarez-Aguirre, N. K. Fontaine, H. Chen, R. A. Correa, Y. Sun, L. Gruner-Nielsen, R. Jensen, R. Lingle, T. Koonen, and C. M. Okonkwo, "138 Tbit/s transmission over 650 km graded-index 6-mode fiber," in *Proc. European Conf. Opt. Commun.*, Sep. 2017, paper Th.PDP.A.4.
- [27] R. Maher, K. Croussore, M. Lauermaier, R. Going, X. Xu, and J. Rahn, "Constellation shaped 66 GBd DP-1024QAM transceiver with 400 km transmission over standard SMF," in *Proc. European Conf. Opt. Commun.*, Sep. 2017, paper Th.PDP.B.2.
- [28] W. Ryan and S. Lin, *Channel Codes: Classical and Modern*. Cambridge University Press, 2009.
- [29] S. Särkkä, *Bayesian Filtering and Smoothing*, 1st ed. Cambridge, UK: Cambridge University Press, 2013.
- [30] C. E. Rasmussen and C. K. I. Williams, *Gaussian Processes for Machine Learning*. Cambridge, MA, USA: The MIT Press, 2006.
- [31] T. P. Minka, "Expectation propagation for approximate bayesian inference," in *Proc. Conf. in Uncertainty in Artificial Intelligence*. San Francisco, CA, USA: Morgan Kaufmann Publishers Inc., Aug. 2001.
- [32] T. M. Cover and J. A. Thomas, *Elements of Information Theory*, 2nd ed. Wiley-Interscience, 2006.
- [33] A. F. Alfredsson *et al.*, "Pilot distributions for phase tracking in space-division multiplexed systems," in *Proc. European Conf. on Opt. Commun.* Optical Society of America, Sep. 2017, paper P1.SC3.48.
- [34] P. Y. Kam, S. S. Ng, and T. S. Ng, "Optimum symbol-by-symbol detection of uncoded digital data over the Gaussian channel with unknown carrier phase," *IEEE Trans. Commun.*, vol. 42, no. 8, pp. 2543–2552, Aug. 1994.